# Ballistic Spin Transport in a Periodically Driven Integrable Quantum System

Marko Ljubotina, Lenart Zadnik,[*] and Tomaž Prosen

*Faculty of Mathematics and Physics, University of Ljubljana, Jadranska 19, SI-1000 Ljubljana, Slovenia*

We demonstrate ballistic spin transport of an integrable unitary quantum circuit, which can be understood either as a paradigm of an integrable periodically driven (Floquet) spin chain, or as a Trotterized anisotropic ($XXZ$) Heisenberg spin-1/2 model. We construct an analytic family of quasilocal conservation laws that break the spin-reversal symmetry and compute a lower bound on the spin Drude weight, which is found to be a fractal function of the anisotropy parameter. Extensive numerical simulations of spin transport suggest that this fractal lower bound is in fact tight.

*Introduction.*—Understanding transport in various out-of-equilibrium setups, in particular, in low dimensions, is one of the main challenges of theoretical condensed matter physics [1]. Experimental evidence corroborates the seemingly controversial proposal [2,3] that integrable systems generically exhibit ballistic transport even at high temperatures [4–6]. This proposal has received rigorous justification in terms of the existence of an extensive number of quasilocal conserved quantities [7–12] which form a basis for the hydrodynamic theory of interacting integrable systems [13–15].

Recently, periodically driven (Floquet) spin chains with local interactions have attracted considerable attention. This was in particular due to the possibility of exhibiting generalized thermalization towards nonequilibrium steady states [16] and distinct dynamical phases with respect to the spontaneous breaking of time-translation invariance [17,18]. Still, the possibility of strictly ballistic transport in interacting quantum integrable Floquet systems has never been explored (see [19,20] for a classical lattice setting), even though a peculiar robustness of transport to integrability breaking was observed a while ago [21,22] (also [23]).

For concreteness, let us consider spin transport. Without resorting to the spectroscopic approach [24], which is harder to justify in Floquet systems, ballistic transport can be defined as a linear growth of the spin current in time, after the system has been prepared in an initial state supporting a small gradient of magnetization. This can be formulated in terms of a nonzero Drude weight,

$$D = \lim_{t\to\infty} \lim_{N\to\infty} \lim_{\mu\to 0} \frac{\langle J(t)\rangle_\mu}{2Nt\mu}, \qquad (1)$$

where $J = \sum_n j_n$ is the extensive spin current operator on a spin chain of length $N$ and $J(t)$ its time dependence. $\langle \bullet \rangle_\mu$ denotes the average in the initial state with a small gradient of magnetization $\mu$, say $\rho_\mu \sim \exp(\mu \sum_n n\sigma_n^z)$, where $\sigma_n^z$ is a local spin variable. A formula similar to (1) holds even if the system is initially prepared in two equilibrated halves at different magnetizations $\mu_L$ and $\mu_R$ with $\mu \sim (\mu_L - \mu_R)/N$ representing the effective gradient [25–27]. This partitioned initial state is easier to simulate using state-of-the-art tensor network simulations.

Expanding to the first order in $\mu$, the Drude weight can be expressed solely in terms of equilibrium autocorrelation functions using the Kubo formula; see Appendix A of the Supplemental material (SM) [28]. This can in turn be bounded from below by means of the Mazur inequality [3,29,30] (see [7] for a rigorous derivation in extended systems),

$$D = \lim_{t\to\infty} \lim_{N\to\infty} \frac{1}{2N} \frac{1}{t} \sum_{\tau=1}^{t} \langle JJ(\tau)\rangle$$
$$\geq \lim_{N\to\infty} \frac{1}{2N} \sum_k \frac{|\langle J, Q_k\rangle|^2}{\langle Q_k, Q_k\rangle}. \qquad (2)$$

Here $Q_k$ are conserved quantities orthogonal with respect to the inner product $\langle A, B\rangle = \text{tr}[A^\dagger B]/2^N$, assuming that the reference equilibrium state is the maximum entropy state $\rho_{\mu=0} = 2^{-N}\mathbb{1}$ and the local Hilbert space dimension is 2. In order for the bound to be finite the conserved quantities should be linearly extensive or quasilocal, $\langle Q_k, Q_k\rangle \propto N$, and should have a finite overlap with the spin current, $\langle J, Q_k\rangle \neq 0$. For the latter to hold, $Q_k$ must not be symmetric, $\mathcal{P}Q_k\mathcal{P} \neq Q_k$, with respect to the spin-reversal operator $\mathcal{P}$, which flips the spin current $\mathcal{P}J\mathcal{P} = -J$. In the easy-plane (gapless) regime of the Heisenberg $XXZ$ model, for example, the integrals of motion with all of the required properties have been shown to exist [8–11].

In the present letter, we aim to rigorously establish a regime of ballistic transport in a Floquet driven integrable model related to the Trotterized $XXZ$ spin-1/2 chain. We introduce the dynamical protocol as a local quantum circuit, establish its connection with the six-vertex $R$-matrix and integrability structure of the $XXZ$ model, and define
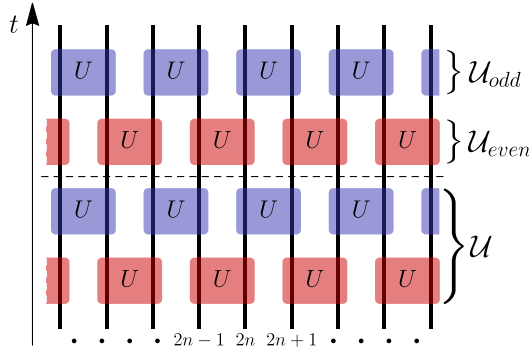
FIG. 1. Schematics of the time evolution. The red gates represent $\mathcal{U}_{\text{even}}$ and the blue ones $\mathcal{U}_{\text{odd}}$. The direction of the time is upwards. The schematic shows two full time steps in the bulk of the system.



FIG. 2. The colored area corresponds to real $\eta$ and imaginary $\lambda$. The blue and yellow lines are constant $\lambda$ and constant $\eta$ contours, respectively. The continuous-time limit corresponds to $\mathcal{J}$, $\mathcal{J}' \to 0$. Note, $\eta = \pi/2$ corresponds to the free model ($\mathcal{J}' = 0$). In the limit $\lambda \to \infty$ ($\mathcal{J} \to \pi/4$) the local propagator (4) reduces to a SWAPlike gate with some $\mathcal{J}'$-dependent phase.

the spin currents and continuity equations arising from the global $U(1)$ symmetry of the model. Despite its driven nature, we construct a set of quasilocal conservation laws that break the spin-reversal symmetry. We then show how to evaluate the optimized Mazur lower bound on the spin Drude weight. Extensive numerical simulations using the time-evolving block decimation (TEBD) algorithm strongly suggest that this bound, which is a fractal function of parameters, is in fact saturated, similarly as in the continuous-time case [27,31].

*The model.*—Consider a spin-1/2 chain with $N \in 2\mathbb{Z}$ sites and periodic boundary conditions. The local physical space on each site is denoted by $\mathcal{V}_p \equiv \mathbb{C}^2$. We are interested in a discrete-time Liouville–von Neumann equation for a density matrix $\rho_{t+1} = \mathcal{U}\rho_t\mathcal{U}^\dagger$. The propagator $\mathcal{U} = \mathcal{U}_{\text{odd}}\mathcal{U}_{\text{even}}$ acts in two steps

$$\mathcal{U}_{\text{odd}} = \prod_{n=1}^{N/2} U_{2n,2n+1}, \qquad \mathcal{U}_{\text{even}} = \prod_{n=1}^{N/2} U_{2n-1,2n}, \quad (3)$$

where

$$U_{n,n+1} = e^{-i\mathcal{J}(\sigma_n^x\sigma_{n+1}^x + \sigma_n^y\sigma_{n+1}^y) - i\mathcal{J}'(\sigma_n^z\sigma_{n+1}^z - 1)} \quad (4)$$

is a unitary gate acting on two neighboring sites labeled with $n$ and $n+1$; see Fig. 1. Here $\sigma^\alpha$ ($\alpha = x, y, z$) are Pauli matrices. By considering infinitesimally small couplings $\mathcal{J}$ and $\mathcal{J}'$ and an infinite number of time steps we recover the continuous-time dynamics of the XXZ model, according to the Trotter-Suzuki formula.

The local two-site unitary gate can be rewritten as $U_{n,n+1} = \check{R}_{n,n+1}(\lambda)$, where

$$\check{R}(\lambda) = \begin{pmatrix} 1 & 0 & 0 & 0 \\ 0 & \frac{\sin\eta}{\sin(\lambda+\eta)} & \frac{\sin\lambda}{\sin(\lambda+\eta)} & 0 \\ 0 & \frac{\sin\lambda}{\sin(\lambda+\eta)} & \frac{\sin\eta}{\sin(\lambda+\eta)} & 0 \\ 0 & 0 & 0 & 1 \end{pmatrix} \quad (5)$$

denotes the braid form of the $R$-matrix of the XXZ model. The new parameters $\eta$ and $\lambda$ can be implicitly expressed as unique functions of $\mathcal{J}$ and $\mathcal{J}'$ through the following pair of relations:

$$e^{2i(\mathcal{J}\pm\mathcal{J}')} = \frac{\sin\eta - \sin\lambda}{\sin(\eta\pm\lambda)}. \quad (6)$$

The continuous-time limit is recovered as an expansion in small $\lambda$, which gives $U_{n,n+1} = \mathbb{1} + \lambda h_{n,n+1} + \mathcal{O}(\lambda^2)$ with the local Hamiltonian density

$$h_{n,n+1} = \frac{1}{2\sin\eta}(\sigma_n^x\sigma_{n+1}^x + \sigma_n^y\sigma_{n+1}^y + \Delta(\sigma_n^z\sigma_{n+1}^z - \mathbb{1})), \quad (7)$$

with $\Delta = \cos\eta$ being the anisotropy parameter. Clearly, real $\eta$ and imaginary $\lambda$ correspond to the gapless or easy-plane regime, shown in Fig. 2, whereas imaginary $\eta$ and real $\lambda$ correspond to the gapped or easy-axis regime.

In the gapless regime of the continuous-time limit ($|\Delta| < 1$) the Drude weight has rigorously been shown to be nonzero for a dense set of anisotropies parametrized by $\eta = l\pi/m$, where $l$ and $m$ are coprime integers [9,10]. In this letter we extend this discussion for the same set of anisotropies to a discrete time, i.e., to all imaginary $\lambda$. This covers the ballistic regime in the phase diagram of our model, shown in red in Fig. 3, which is determined by adapting the numerical method of Ref. [32]. We stress that we observe ballistic transport for any ratio $\mathcal{J}'/\mathcal{J}$, even for $|\mathcal{J}'| > |\mathcal{J}|$, unlike in the continuous-time case. Note also that the other two transport regimes can be clearly
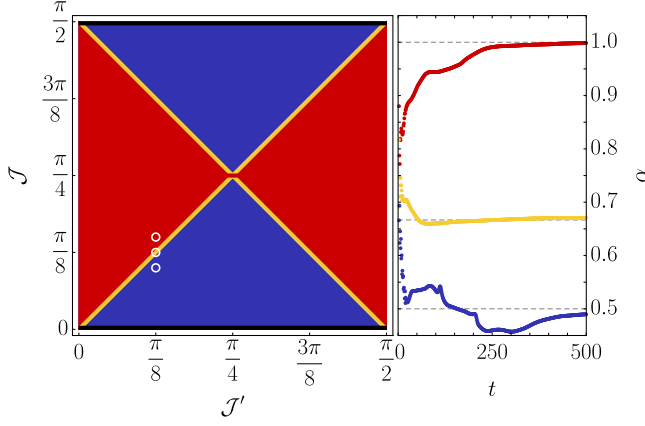
FIG. 3. A schematic phase diagram of the model based on TEBD simulations. The three circles mark the values of $\mathcal{J}$ and $\mathcal{J}'$ used in the right plot, which in turn depicts the time dependence of the exponent $\alpha$, defined through the transport of magnetization between two half-chains [32] $\alpha(t) = (d/d \log t) \log \left( \sum_{\tau=0}^{t} \langle j_{N/2+1}(\tau) \rangle \right)$. We can recognize ballistic, superdiffusive and diffusive regimes (red, yellow, and blue, respectively). Here we have used bond dimension 64 on a chain of length $N = 3600$.

established numerically—the superdiffusive in yellow and the diffusive in blue.

*Spin currents.*—Because of the $U(1)$ symmetry of the propagator (5) the total magnetization $M = \sum_{n=1}^{N} \sigma_n^z$ is a conserved quantity. As a result of the discrete time propagation we identify two continuity equations, separately for odd and even sites,

$$\mathcal{U}^\dagger \sigma_{2n+1}^z \mathcal{U} - \sigma_{2n+1}^z = -j_{2n+2} + j'_{2n+1},$$
$$\mathcal{U}^\dagger \sigma_{2n}^z \mathcal{U} - \sigma_{2n}^z = -j'_{2n+1} + j_{2n}. \quad (8)$$

Through them we can define two local current densities, the even current $j_{2n}$ and the odd, $j'_{2n+1}$. The even one is

$$j_{2n} = \frac{4 \sin \lambda \sin \eta}{\cos 2\eta - \cos 2\lambda} (\sigma_{2n-1}^+ \sigma_{2n}^- - \sigma_{2n-1}^- \sigma_{2n}^+)$$
$$+ \frac{2(\sin \lambda)^2}{\cos 2\eta - \cos 2\lambda} (\sigma_{2n-1}^z - \sigma_{2n}^z), \quad (9)$$

while the odd current can be computed as $j'_{2n+1} = \mathcal{U}^\dagger_{\text{even}} j_{2n+1} \mathcal{U}_{\text{even}}$ and operates on four adjacent sites. In the continuous-time limit both local currents reduce to

$$j_n = j'_n = -\frac{2\lambda}{\sin \eta} (\sigma_{n-1}^+ \sigma_n^- - \sigma_{n-1}^- \sigma_n^+) + \mathcal{O}(\lambda^2), \quad (10)$$

with the prefactor $(\sin \eta)^{-1}$ coming from the Hamiltonian (7).

The total extensive spin current is now defined as $J = \sum_{n=1}^{N/2} (j_{2n} + j'_{2n+1})$. It is clearly antisymmetric under spin reversal $\mathcal{P} = \prod_{n=1}^{N} \sigma_n^x$, i.e., $\mathcal{P} J \mathcal{P} = -J$. We now

proceed to construct the relevant conservation laws for all imaginary $\lambda$ and for a dense set of commensurate values of the anisotropy parameter $\eta = l\pi/m$.

*Quasilocal integrals of motion.*—The construction of antisymmetric conservation laws is similar as in the continuous-time limit [10]. However, due to the two-step staggered propagation, they are now generated by the staggered transfer operator

$$T(\varphi, s) = \text{tr}_a \left[ \prod_{n=1}^{N} \mathbf{L}_{n,a} \left( \varphi - (-1)^n \frac{\lambda}{2}, s \right) \right]. \quad (11)$$

Here, $\mathbf{L}_{n,a}(\varphi, s)$ denotes the Lax operator acting on the $n$th physical space $\mathcal{V}_p$ in the string $\bigotimes_{n=1}^{N} \mathcal{V}_p$ as a $2 \times 2$ matrix

$$\mathbf{L}(\varphi, s) = \frac{1}{\sin \varphi} \begin{pmatrix} \sin(\varphi + \eta \mathbf{S}_s^z) & \sin(\eta) \mathbf{S}_s^- \\ \sin(\eta) \mathbf{S}_s^+ & \sin(\varphi - \eta \mathbf{S}_s^z) \end{pmatrix} \quad (12)$$

whose elements are themselves matrices in the auxiliary space $\mathcal{V}_a$. For $\eta = l\pi/m$ the latter is an $m$-dimensional complex spin-$s$ representation of the quantum group $\mathcal{U}_q(sl_2)$ $(q = e^{i\eta})$ traced out in the final expression (11). Its generators have an explicit form reminiscent of the angular momentum generators

$$\mathbf{S}_s^z = \sum_{k=0}^{m-1} (s-k)|k\rangle\langle k|,$$

$$\mathbf{S}_s^+ = \sum_{k=0}^{m-2} \frac{\sin(k+1)\eta}{\sin \eta} |k\rangle\langle k+1|,$$

$$\mathbf{S}_s^- = \sum_{k=0}^{m-2} \frac{\sin(2s-k)\eta}{\sin \eta} |k+1\rangle\langle k|. \quad (13)$$

Together with $\check{R}(\lambda)$ given in (5), the Lax operator (12) satisfies the Yang-Baxter equation, which implies $[T(\varphi, s), \mathcal{U}] = 0$ and $[T(\varphi, s), T(\varphi', s)] = 0$ (see Appendixes B and C of the SM [28]).

For $\lambda = 0$ the spin-reversal asymmetric conservation laws of the $XXZ$ spin-1/2 chain were previously produced [9–11] as

$$Z(\varphi) = \frac{1}{2\eta \sin \eta} \partial_s T(\varphi, s)|_{s=0}, \quad (14)$$

and shown to be linearly extensive (quasilocal) inside an analyticity strip $|\text{Re}\varphi - \pi/2| < \pi/(2m)$. Here we simply show that this expression can be extended to arbitrary values of parameter $\lambda$ if the staggered form (11) of the transfer matrix is used. Since $\lambda$ is purely imaginary, the region of quasilocality remains the same. The detailed construction of these conservation laws for finite $\lambda$ is presented in Appendix D of the SM [28].

In order to maximize the Mazur lower bound (2) for the spin Drude weight we need to minimize the norm of the conservation laws $Q_k \sim Z(\varphi)$ without reducing the overlap with the spin current $\langle J, Q_k \rangle$. Because of the asymmetry of the current operator $\mathcal{P} J \mathcal{P} = -J$, only the spin-reversal antisymmetric component $Z^-(\varphi) = \frac{1}{2}[Z(\varphi) - \mathcal{P}Z(\varphi)\mathcal{P}]$ contributes to the lower bound. Furthermore, we can subtract a term proportional to the total magnetization, $Z_\perp^-(\varphi) = Z^-(\varphi) - (1/N)\langle M, Z(\varphi)\rangle M$, since the latter is orthogonal to the spin current; see Appendix E of the

SM [28]. The overlap between $Z_\perp^-(\varphi)$ and the current is now given by

$$j(\varphi) = \lim_{N\to\infty} \frac{1}{N}\langle Z(\bar\varphi), J\rangle = \frac{\sin\lambda}{(\cos\lambda - \cos 2\varphi)\sin\eta}. \quad (15)$$

The quasilocality of $Z_\perp^-(\varphi)$ follows from the $N$-independence of $K(\varphi, \varphi') \equiv \lim_{N\to\infty}(1/N)\langle Z_\perp^-(\bar\varphi), Z_\perp^-(\varphi')\rangle$, proven in Appendix F of the SM [28]. There we also conjecture the full, explicit form of $K(\varphi, \varphi')$ to be

$$K(\varphi, \varphi') = \frac{(\cos(\varphi - \varphi' + \lambda) + \cos(\varphi - \varphi' - \lambda) - 2\cos(\varphi + \varphi'))\sin[(m-1)(\varphi + \varphi')] + (\sin\lambda)^2 \sin[m(\varphi + \varphi')]}{4(\sin\eta)^2(\cos 2\varphi - \cos\lambda)(\cos\lambda - \cos 2\varphi')\sin[m(\varphi + \varphi')]}. \quad (16)$$

Expressions (15) for $j(\varphi)$ and (16) for $K(\varphi, \varphi')$ are the essential ingredients for the lower bound on the Drude weight.

*Mazur bound.*—We now attempt to bound the spin Drude weight by means of the Mazur inequality as elaborated on in Ref. [10]. It can be rewritten in an integral form,

$$D \geq D_{\text{Mazur}} = \frac{1}{2}\text{Re}\int d^2\varphi \overline{j(\bar\varphi)} f(\varphi), \quad (17)$$

where $f(\varphi)$ solves the following Fredholm equation:

$$\int d^2\varphi' K(\varphi, \varphi') f(\varphi') = j(\varphi). \quad (18)$$

The integrals are formally taken over the area of quasilocality $|\text{Re}\varphi - \pi/2| < \pi/(2m)$. However, due to holomorphicity, a single line of integration centered at $\text{Re}\varphi = \pi/2$ is sufficient, which makes for an efficient quasiexact numerical procedure of computing $D_{\text{Mazur}}$. The full Mazur lower bound has a fractal dependence on $\eta$ and a continuous dependence on $|\lambda|$. It has been calculated numerically and compared to TEBD [33,34] simulations—see Appendix H of the SM [28]. The dependence on $\eta$ is shown in Fig. 4, and the dependence on $|\lambda|$ in Fig. 5.

In Fig. 4 we have rescaled the Drude weight and the lower bound by a factor of $(\sin\eta)^2$ [see Eq. (7)]. This allows us to make a comparison with the established continuous-time result [10]

$$D'_{\text{Mazur}} = \left(\frac{\sin\eta}{\sin(\pi/m)}\right)^2 \left(1 - \frac{m}{2\pi}\sin(2\pi/m)\right), \quad (19)$$

found by expanding $(\sin\eta)^2 D_{\text{Mazur}} = \lambda^2 D'_{\text{Mazur}} + \mathcal{O}(\lambda^3)$ around $\lambda = 0$. We can see this by noting that the small-$\lambda$ expansion of Eqs. (17) and (18) reproduces the corresponding equations in the continuous-time case.

The integral equations can be solved analytically for $m \to \infty$, corresponding to an irrational value of $\eta/\pi$. The details are discussed in Appendix G of the SM [28] and the result is the enveloping function

$$\lim_{m\to\infty} D_{\text{Mazur}} = 2\left(1 - \frac{\text{Gd}(|\lambda|)}{\sinh(|\lambda|)}\right), \quad (20)$$
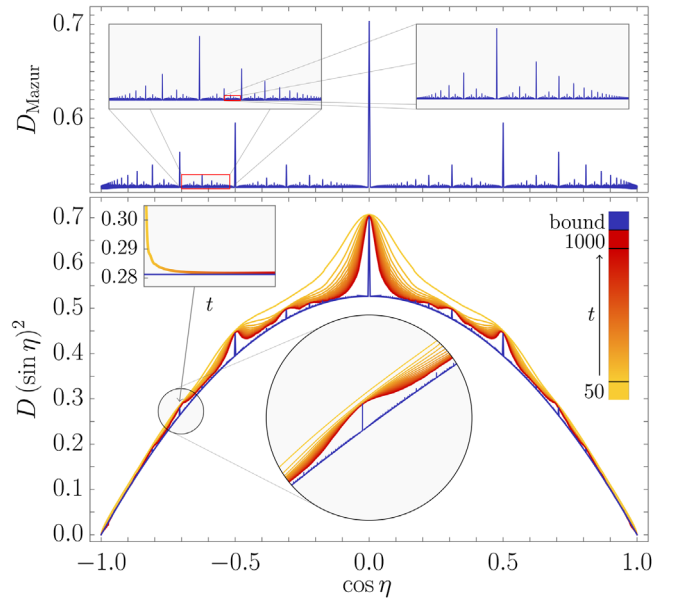


FIG. 4. Drude weight at $|\lambda| = 1$ as computed using the Mazur inequality (blue) and TEBD (yellow-red). The color scales from yellow to red as the simulation time increases from $t = 50$ to $t = 1000$. The TEBD simulations were performed using a bond dimension of 64 and a system size $N = 3600$. The inset in the center of the lower panel shows a more precise set of simulations using a bond dimension of 128 for a small section of $\cos\eta$. The top-left inset of the lower panel shows convergence towards the fractal peak at $\eta = 3\pi/4$ for bond dimension 256. To demonstrate fractality, the upper panel only shows the Mazur bound without the rescaling.
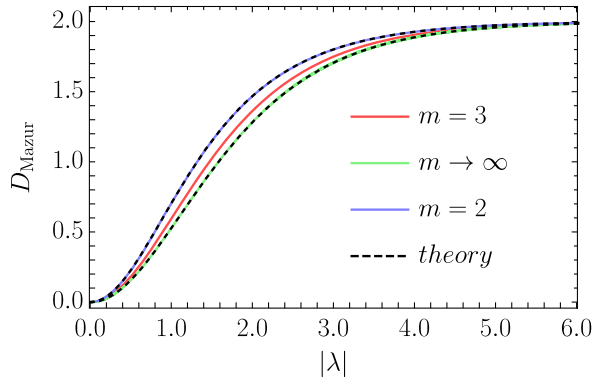
FIG. 5. A comparison between the analytic and numerical results. Additionally we show the $m = 3$ case as an example of more generic behavior with respect to $|\lambda|$. For all $m$, the $|\lambda|$ dependence lies between the $m = 2$ and $m \to \infty$ curves.

where Gd denotes the Gudermannian $\mathrm{Gd}(x) = 2\arctan(e^x) - \pi/2$. This represents a continuous strict lower bound on top of which an additional fractal structure, shown in Fig. 4 for $|\lambda| = 1$, emerges.

On the free fermion line ($\mathcal{J}' = 0$ or $m = 2$) exact diagonalization shows the saturation of the lower bound, which includes only a single conserved quantity $Z(\pi/2)$. It can easily be computed to give

$$D_{\mathrm{Mazur}} = 2[1 - \mathrm{sech}(|\lambda|)]. \tag{21}$$

For a complete $|\lambda|$ dependence of the Mazur lower bound see Fig. 5. Note that the $|\lambda| \to \infty$ limit is always 2. This can easily be explained, since there the local propagator reduces to a SWAP gate. As such, transport becomes perfectly ballistic with no scattering at all.

*Discussion.*—We have demonstrated and proven ballistic transport in a periodically driven interacting quantum spin chain, namely in the Trotterized *XXZ* spin-1/2 model. We have used the notion of ballistic spin transport referring to a linearly growing extensive spin current after a quench from an inhomogeneous initial state with either a linear gradient or a step bias in the magnetization profile. We argue that this is the most natural definition of ballistic transport in the case of discrete-time propagation. Using the quasilocal conservation laws that we constructed by means of quantum-group theoretic methods, we have calculated the lower bound on the spin Drude weight and explicitly shown its fractal dependence on the anisotropy parameter. Extensive numerical simulations suggest the saturation of the lower bound—see Fig. S-2 in Appendix H of the SM. Note, however, that for a fixed commensurate anisotropy $\eta = l\pi/m$ the convergence with time seems to become extremely slow with increasing $m$, certainly beyond ultimate verification with state-of-the-art numerical methods.

In the continuous-time limit we correctly reproduce the well-established results of ballistic spin transport in the *XXZ* model. However, since the thermodynamic Bethe ansatz has not yet been developed for driven integrable systems [35], our results open interesting new avenues for research. The conservation laws that we proposed (see also Ref. [36]) can be directly applied for construction of complete generalized Gibbs ensembles and development of generalized hydrodynamics in integrable Floquet systems.

*Corresponding author.
lenart.zadnik@fmf.uni-lj.si

[1] J. Sirker, R. G. Pereira, and I. Affleck, Phys. Rev. Lett. 103, 216602 (2009); Phys. Rev. B 83, 035115 (2011).
[2] H. Castella, X. Zotos, and P. Prelovšek, Phys. Rev. Lett. 74, 972 (1995).
[3] X. Zotos, F. Naef, and P. Prelovšek, Phys. Rev. B 55, 11029 (1997).
[4] A. V. Sologubenko, T. Lorenz, H. R. Ott, and A. Freimuth, J. Low Temp. Phys. 147, 387 (2007).
[5] J. Simon, W. S. Bakr, R. Ma, M. E. Tai, P. M. Preiss, and M. Greiner, Nature (London) 472, 307 (2011).
[6] C. Hess, C. Baumann, U. Ammerahl, B. Büchner, F. Heidrich-Meisner, W. Brenig, and A. Revcolevschi, Phys. Rev. B 64, 184305 (2001).
[7] E. Ilievski and T. Prosen, Commun. Math. Phys. 318, 809 (2013).
[8] T. Prosen, Phys. Rev. Lett. 106, 217206 (2011).
[9] T. Prosen and E. Ilievski, Phys. Rev. Lett. 111, 057203 (2013).
[10] T. Prosen, Nucl. Phys. B886, 1177 (2014).
[11] R. G. Pereira, V. Pasquier, J. Sirker, and I. Affleck, J. Stat. Mech. (2014) P09037.
[12] E. Ilievski, M. Medenjak, T. Prosen, and L. Zadnik, J. Stat. Mech. (2016) P064008.
[13] B. Bertini, M. Collura, J. De Nardis, and M. Fagotti, Phys. Rev. Lett. 117, 207201 (2016).
[14] O. A. Castro-Alvaredo, B. Doyon, and T. Yoshimura, Phys. Rev. X 6, 041065 (2016).
[15] A. De Luca, M. Collura, and J. De Nardis, Phys. Rev. B 96, 020403(R) (2017).
[16] A. Lazarides, A. Das, and R. Moessner, Phys. Rev. Lett. 112, 150401 (2014).
[17] D. V. Else, B. Bauer, and C. Nayak, Phys. Rev. Lett. 117, 090402 (2016).
[18] V. Khemani, A. Lazarides, R. Moessner, and S. L. Sondhi, Phys. Rev. Lett. 116, 250401 (2016).
[19] K. Klobas, M. Medenjak, T. Prosen, and M. Vanicat, arXiv:1807.05000.
[20] S. Gopalakrishnan, D. A. Huse, V. Khemani, and R. Vasseur, Phys. Rev. B 98, 220303(R) (2018).
[21] T. Prosen, Phys. Rev. Lett. 80, 1808 (1998).
[22] T. Prosen, J. Phys. A 31, L645 (1998); Phys. Rev. E 60, 3949 (1999).

[23] A. Haldar, R. Moessner, and A. Das, Phys. Rev. B **97**, 245122 (2018).

[24] F. Heidrich-Meisner, A. Honecker, D. C. Cabra, and W. Brenig, Phys. Rev. B **68**, 134436 (2003).

[25] R. Vasseur, C. Karrasch, and J. E. Moore, Phys. Rev. Lett. **115**, 267201 (2015).

[26] C. Karrasch, New J. Phys. **19**, 033027 (2017).

[27] E. Ilievski and J. De Nardis, Phys. Rev. Lett. **119**, 020602 (2017).

[28] See Supplemental Material at http://link.aps.org/supplemental/10.1103/PhysRevLett.122.150605 for the derivation of the Kubo form of the Drude weight, review of integrability of the model and demonstration of quasilocality of the conserved operators, as well as the details on the solution of the integral equation and the numerical procedures.

[29] P. Mazur, Physica **43**, 533 (1969).

[30] M. Suzuki, Physica **51**, 277 (1971).

[31] A. Urichuk, Y. Oez, A. Klümper, and J. Sirker, Sci. Post Phys. **6**, 005 (2019).

[32] M. Ljubotina, M. Žnidarič, and T. Prosen, Nat. Commun. **8**, 16117 (2017).

[33] G. Vidal, Phys. Rev. Lett. **91**, 147902 (2003); **93**, 040502 (2004).

[34] U. Schollwöck, Ann. Phys. (Amsterdam) **326**, 96 (2011).

[35] V. Gritsev and A. Polkovnikov, Sci. Post Phys. **2**, 021 (2017).

[36] M. Vanicat, L. Zadnik, and T. Prosen, Phys. Rev. Lett. **121**, 030606 (2018).